GRADED HIERARCHICAL ARCHITECTURE METAMATERIAL IN VIBRATION SUPPRESSION

Akintoye Olumide OYELADE[1], Theddeus T. AKANO[2]

This paper examines two types of graded hierarchical architecture in controlling elastic wave. The metamaterial material is design to have the same resonators but with different configurations; parallel resonators in a host mass and mass in mass in a host mass. The non-dissipative lattice systems for mass in mass systems for the hierarchy level three systems introduces a low-frequency no-pass zone compared to the configurations with a parallel resonator. However, the parallel resonators produce a wider band gap at mid-frequency zone. Therefore, the choice of configurations will be determined by the portion where the stop band is desired. The results in this paper can provide a theoretical basis to design new metaconcrete with enlarged bandgaps to attenuate elastic waves

Keywords: metamaterial, elastic waves, bandgaps, metaconcrete

1. Introduction

Metamaterial has gained traction in engineering and material science due to their unique properties; wave attenuation and tailoring[1–4]. The development in simulation, theoretical, and experimental study on electromagnetic metamaterials has engineered metamaterials with new applications such as under water acoustic, superlensing, cloaking, and, negative refractive indices[5,6]. In taking inspiration from electromagnetic work, researchers in acoustic metamaterials have been able to produce materials and structures that can control and guide the propagation of sound[7,8].

A conventional locally resonant metamaterial has a periodic diatomic microstructure. It is arranged periodically with lumped local resonator embedded in the microstructure. The embedded resonator brings about out of phase motion of the resonator with the host material when the vibration is near the resonance. Hence, negative mass density and the band gap phenomenon occur[9–11]. For illustration, first sonic crystals elastic metamaterial to be fabricated was achieved by a coated lead sphere in an epoxy matrix[12]; a strange bandgap (400–600 Hz) was realized for a small inclusion. The localized resonant structures perform as a structure with effective negative elastic constants and a complete wave reflector within certain

[1] Department of Civil and Environmental Engineering, University of Lagos, Nigeria. e-mail: aoyelade@unilag.edu.ng
[2] Department of Systems Engineering, Faculty of Engineering, University of Lagos, Nigeria

tunable sonic frequency range. A comprehensive review of the metamaterial was presented by Cveticanin and Cveticanin [13].

Metaconcrete has been constructed from the basic principle of metamaterials[14–17]. This is a new type of concrete designed by having the coarse aggregates replaced by engineered inclusions. The conventional metamaterial model was used in all these works to model the metaconcrete. Experiments and analyses have indicated that there was a reduction in the transmission ratio, which is as a result of the concentration of energy within the aggregates near the front of the structures. This caused a reduction in transmitted waves in the range of frequencies where resonant behaviour of aggregates is expected[18].

It is well recognized that the attenuation bandwidth can be enlarged by the use of two or more resonators. First, two resonators were used, and it was demonstrated that acoustic band gap can be created to block wave propagation in several ranges of frequency. The major band gap was determined by the outer mass of the mass-in-mass lattice system[19]. Furthermore, hierarchy two was proposed by Liu and Reina[20] where the detailed parameter study revealed various interesting features of structures with two levels of hierarchy as compared with one level system with identical static mass. Liu and Reina's work showed that the total bandwidth of unit cell two systems is approximately equal, albeit bounded by that of the unit cell one with the same static mass. The combination of different unit cells to form graded designs is a promising avenue for tuning the bandgap structure of acoustic/elastic metamaterials. Also, changing the configuration of the resonators attachment to the host medium can bring about new phenomenon in creating wider broadband. In addition, Guobiao et al [21] investigated two resonators which are coupled through a linear spring. The research focused on the effect of the newly added linear spring on the bandgap and transmittance of the lattice system. Compared to their work, a three level resonators connected in different configurations is investigated.

In this study, we consider two types of graded hierarchical metamaterial of periodic lattice systems with resonant unit cells 3. In the first configuration, the three resonators are connected to the host medium in parallel, whereas in the second configuration, the resonators are embedded in each other. The periodic lattice system is assumed to be non-dissipative. Wave dispersion characteristics of the two configurations with multiple resonators are examined to numerically determine the multiple bandgap formation of the ID system.

2. Theoretical analysis

For standard metamaterials, there are only two positive real solutions. This is expected based on the order of the dispersion equation resulting from the equation. Hence, only one forbidden band gap exists in the system. The dispersion

equation and the effective density of the system in Fig 1. have been given in many references[10,16] as;

$$e^{2i(qx-\omega t)}\begin{bmatrix} 2kk_2-\left(2km_2^j+k_2\left(m_1^j+m_2^j\right)\right)\omega^2 \\ +m_1^j m_2^j\omega^4 \\ -2k\left(k_2-m_2^j\omega^2\right)\cosh\left(iqL\right) \end{bmatrix} \tag{1}$$

$$M_{eff}=M_1+\frac{k_2}{\left(\omega_0^2-\omega^2\right)} \tag{2}$$

where ω is the angular frequency, $\omega_0^2=k_2/m_2$ is the local resonance frequency of m_2, q is the wave number, and L is the length of the unit cell.

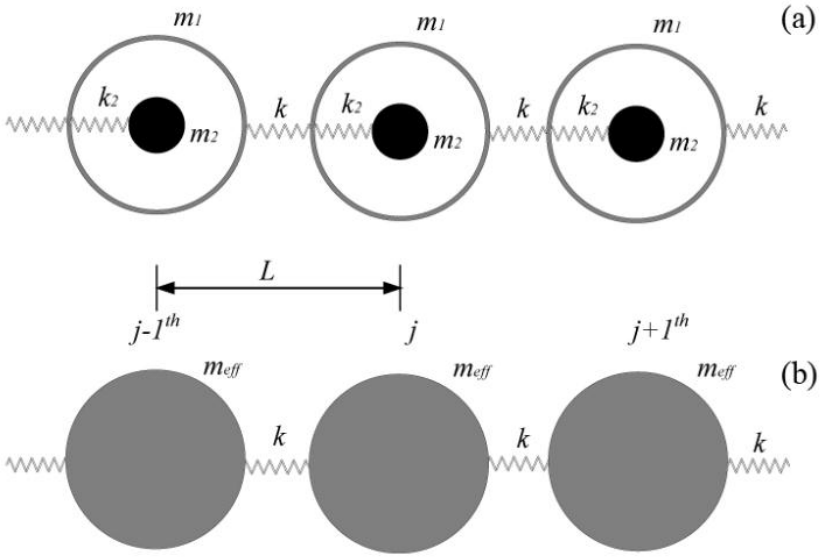

Fig 1. (a) The mass-spring structure with negative effective mass; (b) its equivalent effective model

2.1 1D chain of resonators in parallel

This design of the metamaterial used in this paper is motivated by the work of Liu and Reina[20]. As shown in Fig. 2 (b), the metamaterial consists of three-unit cell. Furthermore, another form of configuration is proposed in Fig. 2(a). In this first case, the other three masses are embedded in mass m as shown in Fig. 2(a).
Applying Newton's second law for the unit cell of the element for Fig 2 (a) gives:

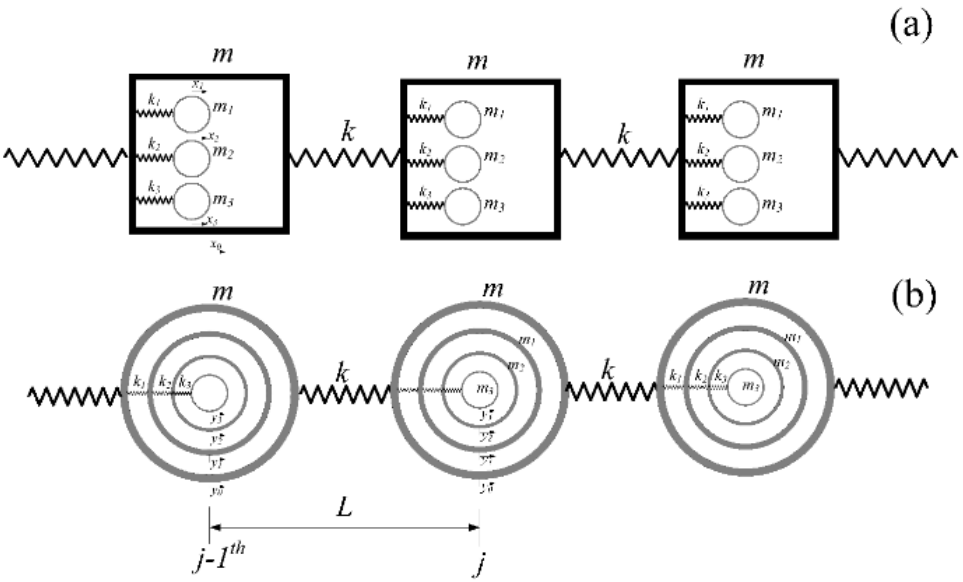

Fig 2. Schematic of 1D mass-spring lattices for (a) three masses embedded in a mass; (b) mass in mass model

$$\begin{aligned} &m\ddot{x}_0^j + k\left(2x_0^j - x_0^{j-1} - x_0^{j+1}\right) + k_1\left(x_0^j - x_1^j\right) \\ &+k_2\left(x_0^j - x_2^j\right) + k_3\left(x_0^j - x_3^j\right) = 0 \end{aligned} \tag{3}$$

$$m_1\ddot{x}_1^j + k_1\left(x_1^j - x_0^j\right) = 0 \tag{4}$$

$$m_2\ddot{x}_2^j + k_2\left(x_2^j - x_0^j\right) = 0 \tag{5}$$

$$m_3\ddot{x}_3^j + k_3\left(x_3^j - x_0^j\right) = 0 \tag{6}$$

The steady state harmonic wave solution for the (j + n)th unit cell is expressed in the form

$$x_\gamma^{(j+n)} = X_\gamma e^{i(j\xi + n\xi - \omega t)} \tag{7}$$

where $\xi = qL$ is the non-dimensional wavenumber, X_γ is complex wave amplitude, q is wave number, ω is angular frequency, and $\gamma = 0,1,2$ and 3. From Eqns. (3) - (7), the determinant of the coefficient matrix of the system of equations is set equal to zero as:

$$\begin{bmatrix} c_{11} & -1 & -\lambda_2 & -\lambda_3 \\ -1 & c_{22} & 0 & 0 \\ -\lambda_2 & 0 & c_{33} & 0 \\ -\lambda_3 & 0 & 0 & c_{44} \end{bmatrix} = 0 \tag{8}$$

where $c_{11} = -\frac{\Omega^2}{\theta_1} + 2\lambda(1 - cos\xi) + 1 + \lambda_2 + \lambda_3, c_{22} = -\Omega^2 + 1$ $c_{33} = -\frac{\Omega^2\theta_2}{\theta_1} + \lambda_2$, $c_{44} = -\frac{\Omega^2\theta_3}{\theta_1} + \lambda_3$, $\Omega = \omega/\omega_0$ is the non-dimensional frequency with $\omega_0 = \sqrt{k_1/m_1}$. The ratio of the masses and stiffness are given as $\theta_1 = m_1/m, \theta_2 = m_2/m, \theta_3 = m_3/m, \lambda = k/k_1, \lambda_2 = k_2/k_1, \lambda_3 = k_3/k_1$

2.2 1D chain of resonators embedded in each other

The second model shown in Fig 2 (b), which is similar to Liu and Reina model is presented here. The equations of motion are given by:

$$m\ddot{y}_0^j + k\left(2y_0^j - y_0^{j-1} - y_0^{j+1}\right) + k_1^0\left(y_0^j - y_1^j\right) = 0 \tag{9}$$

$$m_1\ddot{y}_1^j + k_1\left(y_1^j - y_0^j\right) + k_2\left(y_1^j - y_2^j\right) = 0 \tag{10}$$

$$m_2\ddot{y}_2^j + k_2\left(y_2^j - y_1^j\right) + k_3\left(y_2^j - y_3^j\right) = 0 \tag{11}$$

$$m_3\ddot{y}_3^j + k_3\left(y_3^j - y_2^j\right) = 0 \tag{12}$$

Substituting of the harmonic wave solution into Eqs. (9) - (12) gives the dispersion relations which can be calculated from the determinant of Eqn. (13)

$$\begin{bmatrix} a_{11} & -1 & 0 & 0 \\ -1 & a_{22} & -\lambda_2 & 0 \\ 0 & -\lambda_2 & a_{33} & -\lambda_3 \\ 0 & 0 & -\lambda_3 & a_{44} \end{bmatrix} = 0 \tag{13}$$

Where $a_{11} = -\Omega^2/\theta_1 + 2\lambda(1 - cos\xi) + 1, a_{22} = -\Omega^2 + 1 + \lambda_2,$
$a_{33} = -(\Omega^2\theta_2)/\theta_1 + \lambda_2 + \lambda_3, a_{44} = -(\Omega^2\theta_3)/\theta_1 + \lambda_3$

3. Parametric study

In the parametric investigation for these two configurations, these parameters will be used unless otherwise stated. For the mass and stiffness, $\theta_1 = 4, \theta_2 = 4, \theta_3 = 4, \lambda = 30/4, \lambda_2 = \lambda_3 = 1$. The three mass resonator embedded in a host will be termed Case 1 and mass in mass model will be denoted as Case 2.

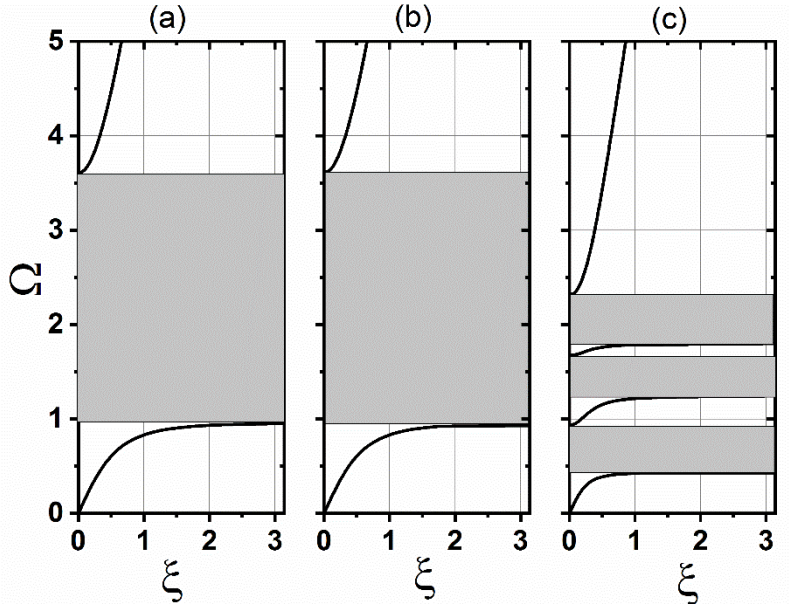

Fig 3. Dispersion curves for periodic one-dimensional lattice structures with: (a) one mass embedded in a mass; (b) three masses embedded in a mass (Case 1); (c) mass in mass model (Case 2)

The non-dimensional wavenumber as a function of frequency is plotted in Fig. 3. The total mass in the three models is equivalent. In Fig. 3 (a) the conventional metamaterials is shown to have bandgap of 0.97- 3.62 Hz, whereas for Case 1, the stop band occurs at 0.91- 3.62 Hz. There is a small discrepancy here because the three resonators are connected at different points in the host material. Therefore, when hierarchy level one and hierarchy level three metamaterial is made to have the same inner mass, the stop band created are similar. The effect of the displacements of the attachments of the resonators does not have much effect on the bandgap. However, there are multiple bandgaps in Case 2 due to different resonators embedded in each other; hence three stop band are created. For wider broadband, using Case 1 may be more effective, whereas when low frequency vibration attenuation is the target for the metamaterial, Case 2 is the preferred configuration. To understand the physics of energy transfer within the inner resonators, the displacement of inner masses, m_2, m_3 and m_4, for Case 1 and Case 2 are calculated from the eigenvectors of Eq. (8) and (13), respectively. The plot of the frequency against the dimensionless displacement for the three resonators is depicted in Fig. 4.

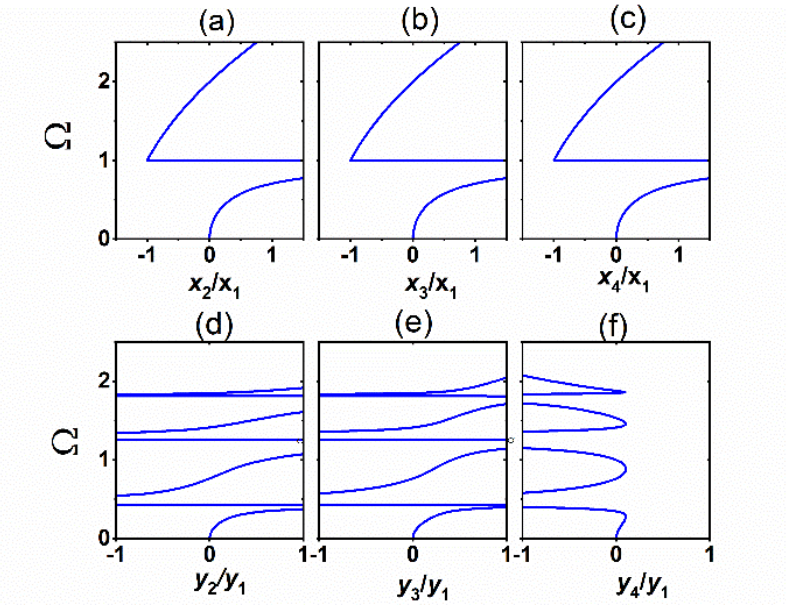

Fig 4. Frequency as a function of dimensionless displacement for m_2, m_3 and m_4 for Case 1 (a) - (c) and for Case 2 (d) - (f)

For Case 1, all the resonators are in phase with the host materials at frequency zero to 1, and after frequency 1, the resonators move in anti-phase. However, for the Case 2, due to the configuration of the system, only two resonators are in phase with the host material at low frequency (0-0.4) while the third resonator moves in anti-phase with the host mass for the given frequency. The band gap is created at the point when the two resonators move in anti-phase with the host material.

The corresponding band edge frequencies diagram is shown in Fig. 5, where the stiffness ratio λ is varied from zero to six. It can be observed that λ value does not change the bandgap edges. Fig. 6 shows the effect of the ratio of the inner stiffness with the stiffness connecting the host mass λ_3. We note for Case 1, in Fig. 6(a) that, with the increase of λ_3 lower and upper edges for the 1st band gap is narrow compared to the wide bandgap in Case 2 as shown in Fig. 6 (c). This is as a result of the coupling of the mass to each other unlike what we have in Case 1, where there is an only coupling of the host mass with the other three masses. However, for the 2nd band gap zone, Case 2 provided wider broadband compared to Case 1 as shown in Fig 6 (d) and (b) respectively.

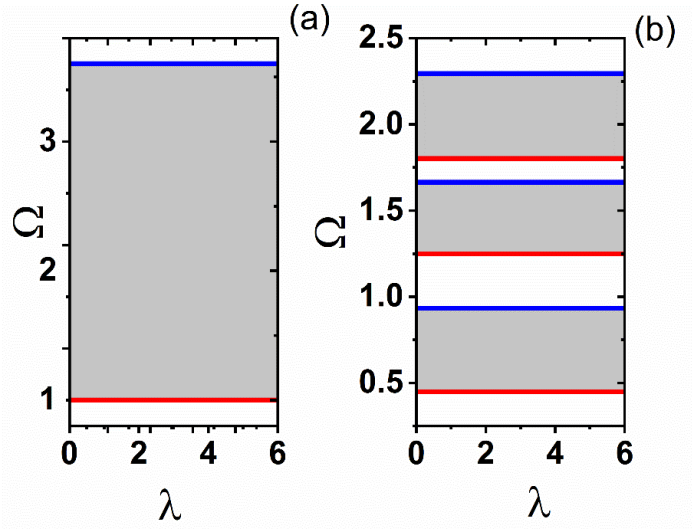

Fig 5. Bandgap variations of the lower and upper edges of the bandgaps for the three resonator lattice system with different λ : (a) Case 1 lower and upper edges for 1st band gap; (b) Case 1 lower and upper edges for 2nd band gap ; (c) Case 2 lower and upper edges for 1st band gap; (d) Case 2 lower and upper edges for 2nd and 3rd band gap.

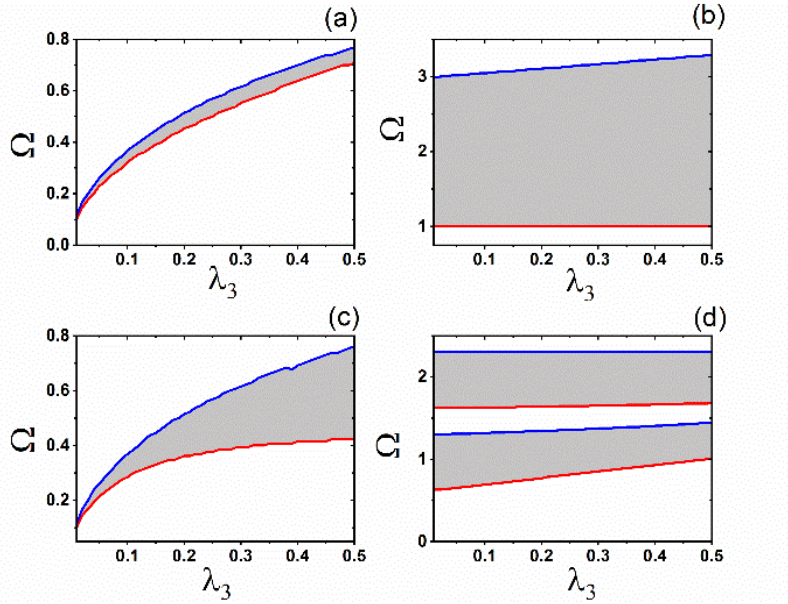

Fig 6. Bandgap variations of the lower and upper edges of the bandgaps for the three resonator lattice system with different λ_3: (a) Case 1 lower and upper edges for 1st band gap; (b) Case 1 lower and upper edges for 2nd band gap ; (c) Case 2 lower and upper edges for 1st band gap; (d) Case 2 lower and upper edges for 2nd and 3rd band gap.

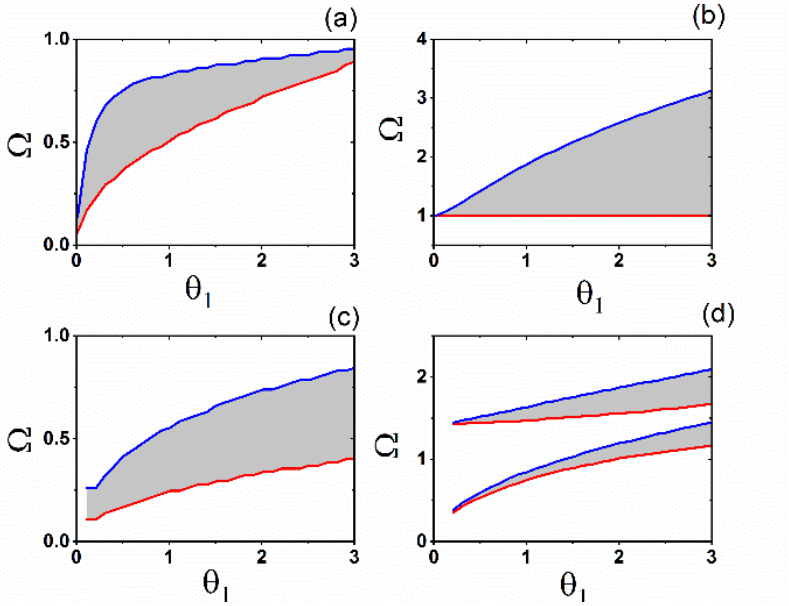

Fig 7. Bandgap variations of the lower and upper edges of the bandgaps for the three resonator lattice system with different θ_1 : (a) Case 1 lower and upper edges for 1st band gap; (b) Case 1 lower and upper edges for 2nd band gap ; (c) Case 2 lower and upper edges for 1st band gap; (d) Case 2 lower and upper edges for 2nd and 3rd band gap.

We are now ready to inspect the effect of the mass ratio θ_1 on the overall bandwidth of the two configurations. The dependency of the mass ratio θ_1 against frequency is plotted in Fig. 7. The bandgap increases from $\theta_1 = 0.1$ to $\theta_1 = 3$, corresponding to Case 2, as shown in Fig. 7 (c), while for Case 1, the bandgap increases as θ_1 increases to an extent but tend to reduce as θ_1 reaches 1 for the 1st band gap (Fig 7 (a)). There is a linear relationship between the mass ratio and frequency for the 2nd bandgap for Case 1 as shown in Fig. 7 (b). This is different from the characteristics of bandgap formation for Case 2, where there are two narrow bandgaps.

4. Conclusions

This paper has presented two configurations of graded designs for tuning the bandgap structures of acoustic/elastic metamaterials. The results show that the total bandwidth of multiple resonator systems for Case 1 is roughly equal with that of the single-resonator unit with the same static mass. When the host material housed the multiple resonators as we have in Case 1, there is broad wave attenuations at relatively high frequencies. In contrast to Case 2, where the mass is inserted in each other, which produces narrow bandgap at low frequencies. These two configurations can be used in many applications such as in rainbow trapping devices and low frequency bending waveguides.

REFERENCES

[1] *X. Zhou, G. Hu,* Analytic model of elastic metamaterials with local resonances, Phys. Rev. B - Condens. Matter Mater. Phys. B 79, (2009) 1–9. doi:10.1103/PhysRevB.79.195109.

[2] *G. Ma, C. Fu, G. Wang, P. del Hougne, J. Christensen, Y. Lai, P. Sheng,* Polarization bandgaps and fluid-like elasticity in fully solid elastic metamaterials, Nat. Commun. 7 (2016) 13536. doi:10.1038/ncomms13536.

[3] *P. Taylor, H.H. Huang, C.T. Sun*, Locally resonant acoustic metamaterials with 2D anisotropic effective mass density, (2011) 37–41. doi:10.1080/14786435.2010.536174.

[4] *N.I. Zheludev*, The Road Ahead for Metamaterials, Science (80-.). 328 (2010) 582–583. doi:10.1126/science.1186756.

[5] *S.A. Cummer, D. Schurig*, One path to acoustic cloaking, New J. Phys. 9 (2007) 45. doi:10.1088/1367-2630/9/3/045.

[6] *X. Zhou, G. Hu, X. Zhou, G. Hu*, Superlensing effect of an anisotropic metamaterial slab with near-zero dynamic mass Superlensing effect of an anisotropic metamaterial slab with near-zero dynamic mass, Appl. Phys. Lett. 98 (2012) 263510. doi:10.1063/1.3607277.

[7] *X.N. Liu, G.K. Hu, C.T. Sun, G.L. Huan*g, Wave propagation characterization and design of two-dimensional elastic chiral metacomposite, J. Sound Vib. 330 (2011) 2536–2553. doi:10.1016/j.jsv.2010.12.014.

[8] *R. Zhu, X.N. Liu, G.K. Hu, C.T. Sun, G.L. Huang*, A chiral elastic metamaterial beam for broadband vibration suppression, J. Sound Vib. 333 (2014) 2759–2773. doi:10.1016/j.jsv.2014.01.009.

[9] *S. Yao, X. Zhou, G. Hu*, Experimental study on negative effective mass in a 1D mass–spring system, New J. Phys. 10 (2008) 043020. doi:10.1088/1367-2630/10/4/043020.

[10] *X. Zhou, X. Liu, G. Hu*, Elastic metamaterials with local resonances: an overview, Theor. Appl. Mech. Lett. 2 (2012). doi:10.1063/2.1204101.

[11] *J. Li, C.T. Chan*, Double-negative acoustic metamaterial, Phys. Rev. E - Stat. Nonlinear, Soft Matter Phys. 70 (2004) 055602. doi:10.1103/PhysRevE.70.055602.

[12] *Z. Liu, X. Zhang, Y. Mao, Y.Y. Zhu, Z. Yang, C.T. Chan, P. Sheng*, Locally resonant sonic materials, Science (80-.). 289 (2000) 1734–1736. doi:10.1126/science.289.5485.1734.

[13] *L. Cveticanin, D. Cveticanin*, Application of the acoustic metamaterial in engineering: An overview, Rom. J. Mech. 2 (2017) 29–36. http://ejournal.bsi.ac.id/ejurnal/index.php/paradigma/article/view/2306/1615.

[14] *S. Mitchell,* Metaconcrete : engineered aggregates for enhanced dynamic performance, 2015.

[15] *S.J. Mitchell, A. Pandolfi, M. Ortiz*, Metaconcrete: Designed aggregates to enhance dynamic performance, J. Mech. Phys. Solids. 65 (2014) 69–81. doi:10.1016/j.jmps.2014.01.003.

[16] *A.O. Oyelade, Y.O. Abiodun, O.M. Sadiq*, Dynamic behaviour of concrete containing aggregate resonant frequency, J. Comput. Appl. Mech. 49 (2018) 175–180. doi:10.22059/jcamech.2018.269048.339.

[17] *S.J. Mitchell, A. Pandolfi, M. Ortiz,* Investigation of elastic wave transmission in a metaconcrete slab, Mech. Mater. 91 (2015) 295–303. doi:10.1016/j.mechmat.2015.08.004.

[18] *D. Briccola, M. Ortiz, A. Pandolfi,* Experimental Validation of Metaconcrete Blast Mitigation Properties, J. Appl. Mech. 84 (2016) 031001. doi:10.1115/1.4035259.

[19] *G.L. Huang, C.T. Sun*, Band gaps in a multiresonator acoustic metamaterial, J. Vib. Acoust. Trans. ASME. 132 (2010) 0310031–0310036. doi:10.1115/1.4000784.

[20] *C. Liu, C. Reina*, Broadband locally resonant metamaterials with graded hierarchical architecture, J. Appl. Phys. 123 (2018) 095108. doi:10.1063/1.5003264.

[21] *G. Hu, L. Tang, R. Das, S. Gao, H. Liu*, Acoustic metamaterials with coupled local resonators for broadband vibration suppression, AIP Advances. 7 (2017) 025211.